Research Square

Preprints are preliminary reports that have not undergone peer review.
They should not be considered conclusive, used to inform clinical practice,
or referenced by the media as validated information.

Miniaturised multiplex ddPCR determination of rRNA-based biomarkers to complement high-throughput Mycobacterium tuberculosis drug-response profiling

Juan Calvet-Seral
jcalvet@ing.uc3m.es
Universidad Carlos III de Madrid
Lidia de Tapia-Hernández
Universidad Carlos III de Madrid
Lucía Yubero-Fernandez
Universidad Carlos III de Madrid
Patricio Roberto López-Expósito
Universidad Carlos III de Madrid
Francisco de Dios-Antón
Universidad Carlos III de Madrid
Juan José Vaquero
Universidad Carlos III de Madrid
Pablo Catalán-Fernandez
Universidad Carlos III de Madrid
Santiago Ferrer-Bazaga
Universidad Carlos III de Madrid
Alfonso Mendoza-Losana
Universidad Carlos III de Madrid

Article

Keywords: Tuberculosis, Mycobacterium tuberculosis, mycobacteria, molecular biomarkers, RS-ratio, drug characterisation.

Posted Date: November 23rd, 2026

DOI: https://doi.org/10.21203/rs.3.rs-11598011/v1

License: This work is licensed under a Creative Commons Attribution 4.0 International License. Read Full License

Additional Declarations: No competing interests reported.

Abstract

Ribosomal RNA (rRNA)-based biomarkers can complement conventional phenotypic and culture-based readouts by providing information on bacterial burden and ongoing ribosomal biogenesis. However, RNA workflows limit their use in medium- to high-throughput *in vitro Mycobacterium tuberculosis* (*Mtb*) drug studies.

We developed a multiplexed droplet digital PCR assay that simultaneously quantified two precursor-rRNA targets, ETS1 and ITS1, two total-rRNA targets, 16S and 23S rRNA, and an exogenous RNA control. The workflow was miniaturised to process samples from 96-well drug-response assays, including a heat-inactivation procedure enabling downstream RNA processing outside BSL-3 facilities. The platform was evaluated using *Mtb* H37Ra exposed to ten treatment conditions at eight concentrations, integrating resazurin conversion, CFUs, MPNs, rRNA burden, and RS-ratio measurements.

The different readouts produced distinct and complementary drug-response profiles. Principal component and correlation analyses separated the RS-ratios from growth-, culturability-, and burden-associated readouts. The multiplexed assay allowed us to assess redundancy within each molecular biomarker class by providing two rRNA-burden measurements based on 16S and 23S rRNA and four RS-ratio combinations, with ETS1/23S providing the widest dynamic range.

This workflow enables complementary molecular, phenotypic, and culture-based drug-response profiling from the same 96-well samples and supports future evaluation of antitubercular drugs and combinations.

Introduction

Tuberculosis (TB), caused by different members of the *Mycobacterium tuberculosis* (*Mtb*) complex, is the deadliest infectious disease in human history [1]. Although TB is treatable with antibiotics and the number of attributable deaths has declined in recent decades, the latest report still estimates that 1.23 million people died in 2024 due to this disease [2]. TB treatment involves a multi-antibiotic approach over a prolonged period. The most widely used regimen for drug-susceptible TB consists of two months of daily/continuous dosing with four antibiotics (Rifampicin, RMP; Isoniazid, INH; Ethambutol, EMB; and Pyrazinamide, PZN), followed by a four-month continuation phase with two of them (RMP and INH). This regimen has saved millions of lives in recent decades, with an ≈ 85% success rate for drug-susceptible *Mtb* strains. However, the emergence and propagation of drug-resistant strains pose a significant threat to global health. Current treatment regimens for these strains necessitate protracted courses of antibiotic combinations with frequent side effects that patients often find challenging to tolerate. Although shorter all-oral regimens containing bedaquiline (BDQ), pretomanid (PA-824), linezolid (LZD), and sometimes moxifloxacin (MXF), known as BPaL and BPaLM regimens, have improved treatment options for multidrug- or RMP-resistant TB, access remains limited and global treatment success remains lower than for drug-susceptible disease [2]. To improve these outcomes, new antibiotics and combinations must be developed. To achieve this challenging objective, there is a need for improved tools capable of characterising drug combinations more holistically across the different stages of the drug development pathway, ranging from *in vitro* assays to clinical trials.

Within the European Regimen Accelerator for Tuberculosis (ERA4TB) consortium [3], a substantial effort is underway to further develop and implement state-of-the-art technologies for characterising drug combinations against TB, with a particular emphasis on the *in vitro* assays, which enable broader testing than animal studies or clinical trials while imposing fewer ethical constraints. The *in vitro* activities encompass a range of assays, including growth inhibition assays at a fixed time point, akin to the standard minimal inhibitory concentration (MIC) determination measured by optical density or after the addition of redox-growth indicators like resazurin or Methyl Thiazolyl Tetrazolium (MTT). Moreover, time-kill assays (TKAs) are performed as longitudinal assays to determine the bactericidal potential of the drugs, measuring *Mtb* viability by colony-forming units (CFUs) on agar plates and the most probable number (MPN) of differentially culturable *Mtb* by serial dilution in broth. The capacity of TKAs is frequently constrained by the need to test different culture conditions in flasks. However, ERA4TB has successfully adapted TKAs to 96-well plate formats, allowing efficient CFU and MPN determination over time [4]. Furthermore, the Optimised Time Kill Assay (OPTIKA) workflow has increased the throughput of longitudinal kill-kinetic evaluation in 96-well formats [5].

Recently, novel molecular biomarkers have been implemented to assess *Mtb* treatment response, with a focus on their application in animal experiments and the clinic. The molecular bacterial load assay (MBLA) aims to estimate the bacterial burden present in sputum samples by quantifying the amount of 16S ribosomal RNA (rRNA) of *Mtb* present in the sample [6, 7]. An exogenous control (EC) RNA is added to the samples to normalise quantification among them, using RT-qPCR. A similar approach has also been published for its application to mouse lung necropsy samples, though reporting directly the concentration of rRNA (rRNA burden) instead of estimated CFUs [8]. The rRNA synthesis ratio (RS-ratio) compares the amount of precursor rRNA (pre-rRNA) relative to the 23S rRNA of *Mtb*, and it reflects changes in ongoing rRNA biogenesis [9]. A decline in the RS-ratio from necropsies has been demonstrated to be associated with a reduced incidence of relapse in murine TB models. The RS-ratio has also been applied in sputum samples; however, *in vitro*, it has been used only in low-throughput drug monotherapy studies. To date, rRNA burden and RS-ratio have not been applied to large-scale *in vitro* studies.

In the present investigation, we developed a single-tube multiplex ddPCR assay for simultaneous rRNA burden and RS-ratio determination, miniaturised the workflow for 96-well drug-response assays, validated sample inactivation to allow sample processing outside biosafety level 3 (BSL-3) facilities, and evaluated its compatibility with conventional phenotypic and culture-based readouts. The successful application of these biomarkers in conjunction with the classical readouts would facilitate the acquisition of relevant physiological information on drug (and combination) effects, with the potential to expedite *in vitro* studies and improve decision-making during drug and combination evaluation.

Results

Development and Optimisation of a Multiplexed ddPCR Assay. The primary initial objective was the creation of a single-tube multiplexed droplet digital PCR (ddPCR) assay for the determination of both the rRNA burden and the RS-ratio concurrently. This approach aimed to eliminate the need for separate

reactions to measure rRNA burden (traditionally 16S rRNA) and RS-ratio (traditionally 23S rRNA and a pre-rRNA target). The Bio-Rad QX600 ddPCR system's high precision, low limit of detection, and multi-channel capabilities have been exploited in the design of a single-tube assay able to quantify five key targets simultaneously: I) ETS1 and ITS1 sequences for pre-rRNA quantification, II) 16S and 23S rRNA for total rRNA burden determination **(**Fig. 1a**)**, and III) a specific sequence from *Solanum tuberosum* (*phyB* gene) as EC RNA **(**Fig. 1b**)** to control RNA extraction and cDNA synthesis efficiency. We sourced the published primer and probe sequences for these targets and adapted their fluorophores to ensure distinct detection in the five available channels of the QX600 system. In order to validate the specificity, the detection of *Mtb* and EC targets was tested against genomic DNA from *Mtb*, *S. tuberosum*, and two other mycobacterial species, *M. smegmatis* and *M. ulcerans* **(**Fig. 1c**)**. The results of the specificity tests confirmed the reliable and specific amplification of the *Mtb* ETS1, 23S rRNA, and the EC RNA targets. However, the *Mtb* ITS1 and 16S rRNA primer/probe sets exhibited nonspecific cross-amplification when tested with genetic material from *M. ulcerans*. Notwithstanding these cross-amplification results, the five oligonucleotide sets demonstrated robust performance with our primary target, *Mtb*. Consequently, they were employed throughout the study to investigate the influence of different targets on rRNA burden and RS-ratio determination.

Implementation of a High-Throughput RNA Extraction and Sample Inactivation Protocol. Following the successful validation of our multiplexed ddPCR assay, we addressed a major impediment to its extensive deployment in large-scale *in vitro* experiments: the incompatibility of conventional RNA extraction methods in terms of volume. Most commonly used protocols require sampling of 1–10 mL of culture (Fig. 2a), a volume that is prohibitive for modern drug screens—such as MIC determinations or TKAs within the ERA4TB consortium—which operate in 96-well plates with restricted total volumes of approximately 200 µL. In order to overcome this physical limitation, a protocol specifically adapted to these formats was developed. The method involves the direct sampling of a minimal volume of culture (50 µL) and transferring it to a PCR plate well prefilled with 150 µL of DNA/RNA Shield (DRSh) (Fig. 2b). This procedure enables molecular monitoring that respects the limited volume available in large antibiotic evaluation assays without draining the bacterial culture.

Beyond its role in streamlining the workflow, a rigorous investigation was conducted into the sample inactivation properties of DRSh. Although TRIzol is known to inactivate *Mtb* (30 min of incubation at room temperature is sufficient to sterilise a sample, Fig. 2c), the safety profile of DRSh for *Mtb* required careful assessment. It was previously demonstrated that DRSh reduces *Mtb* viability by more than 4 $\log_{10}$ [10], and the manufacturer claims complete inactivation. Despite confirming a > 4 $\log_{10}$ reduction in *Mtb* H37Ra viability (**Supplementary Figure S1**), our tests showed that a 30 min room-temperature incubation of a high-titer *Mtb* H37Ra suspension (≈ 1.4×10^8 CFUs/mL) with three volumes of DRSh was not sufficient for complete inactivation of the sample. Despite the absence of growth in the initial broths, turbidity was observed, indicating bacterial growth in the 1:100 dilution by extending the incubation period to over 40 days. This finding underscores a potential biohazard risk for samples handled or shipped outside of BSL-3 facilities.

Consequently, two heat treatments were tested to ensure complete inactivation: incubation at 80°C for 30 min or at 99°C for 5 min. The application of both methods to samples in either DRSh or PBS reliably achieved complete sterilisation (Fig. 2c). This volume and procedure allow for the sampling of 50 µL of *Mtb* cultures from a 96-well plate and their inactivation with 150 µL of DRSh in a conventional thermocycler while protecting the samples from degradation. This process facilitates the secure storage, shipping, and processing of samples in external facilities, thereby minimising the risk of biohazard exposure.

Finally, to validate the entire workflow, sequential 10-fold dilutions of *Mtb* H37Ra (50 µL each) were processed in 150 µL of DRSh containing a constant amount of external control RNA (≈ 10^8 copies) (Fig. 2d). Following inactivation at 80°C, RNA extraction and cDNA synthesis, quantification was performed using our multiplexed ddPCR assay. As expected, a linear decrease in bacterial rRNA was observed, while the external control remained constant (Fig. 2e and 2f). These results confirm the successful implementation of a high-throughput, efficient, and safe protocol for determining both rRNA burden and RS-ratio from *in vitro Mtb* samples.

Proof-of-concept of high-throughput drug characterisation assays. To demonstrate the compatibility of our high-throughput protocol with additional biomarkers, we conducted a proof-of-concept drug-response experiment. *Mtb* H37Ra was incubated with ten distinct antitubercular treatment conditions, each evaluated at eight different concentrations across three independent replicates using 96-well plates. From these samples, we assessed five complementary biomarkers, or readout classes, to analyse the bacterial response to drug exposure: 1) rRNA burden and 2) RS-ratio, using our newly developed multiplexed ddPCR assay, 3) resazurin fluorescence conversion assessed visually for MIC determination and quantified by fluorescence for multivariate analysis, 4) colony-forming units (CFUs) to quantify culturable bacteria, and 5) the Most Probable Number (MPN) to quantify differentially culturable bacteria. Because rRNA burden was calculated using either 16S or 23S rRNA and the RS-ratio using four precursor-to-total-rRNA combinations, these five readout classes generated nine quantitative variables for subsequent multivariate analysis.

Notably, responses to the different pharmacological agents varied according to both the drug and the readout (Figs. 3 and 4). Concerning the various determinations of rRNA burden and RS-ratio (Figs. 3 and 4, rows 3 and 4, respectively), rRNA burden profiles were similar whether calculated using 23S or 16S rRNA (Figs. 3 and 4, row 3). Comparable profiles were also observed among the four RS-ratio determinations, with similar trends obtained when comparing either ETS1 or ITS1 against 23S or 16S rRNA. However, for those drugs that reduce the RS-ratio, the greatest dynamic range was observed when employing the ETS1/23S rRNA pair (Figs. 3 and 4, row 4).

The MIC of MXF was determined to be 0.025 µg/mL. The CFUs, MPNs, and rRNA burden progressively declined across the concentration range tested. The CFUs reached the lower limit of quantification (LLQ; 400 CFUs/mL) at ≥ 0.1 µg/mL, and the MPN LLQ (15 MPNs/mL) at 1.6 µg/mL, although some culturable bacteria remained detectable at 6.4 µg/mL. The 23S and 16S rRNA burdens also gradually decreased at concentrations ≥ 0.00625 µg/mL, with a marked reduction from 1×10^{11} to 1×10^9 copies/mL at 0.025 µg/mL, followed by a progressive reduction to 3×10^8 copies/mL at 6.4 µg/mL. MXF reduced the RS-ratio from ≈ 600–900 at subinhibitory concentrations and untreated control conditions to ≈ 100 at ≥ 0.1 µg/mL. Surprisingly, the lowest RS-ratio values (≈ 20–40) were observed at 0.1 µg/mL, followed by a partial recovery to ≈ 100 at the highest concentrations tested (Fig. 3, **column 1**).

Across the tested RMP range (12.8 to 0.000781 µg/mL), no resazurin conversion was observed, consequently, the MIC could not be determined in this experiment. Nevertheless, low numbers of culturable bacteria remained detectable, either by CFUs (≈ 1×10^3 CFUs/mL) or MPNs (≈ 1×10^2-1×10^4 MPNs/mL) at concentrations ≤ 3.2 µg/mL. The rRNA burden remained consistent (≈ 3–6 × 10^8 copies/mL) across the concentrations tested, whereas the RS-ratio was partially reduced (≈ 100) at 0.000781 µg/mL, reaching the strongest reduction (≈ 3–20) at ≥ 0.0031 µg/mL (Fig. 3, **column 2**).

The MIC of BDQ was found to be 0.1 µg/mL. Across the range of concentrations tested, from 6.4 µg/mL to 0.0004 µg/mL, we observed a gradual decline in bacterial load, evidenced by CFUs decreasing (from ≈ 5×10^5 to ≈ 3×10^3 CFUs/mL) and MPNs dropping (from ≈ 8×10^6 to ≈ 7×10^3 MPNs/mL). The rRNA burden also exhibited a gradual decline (from ≈ 1×10^{11} to ≈ 1×10^9 copies/mL) over a smaller range of concentrations (0.4 to 0.0063 µg/mL). Additionally, the RS-ratio showed a gradual reduction at concentrations > 0.4 µg/mL, decreasing to ≈ 30 at 6.4 µg/mL (Fig. 3, **column 3**).

The determined MIC for streptomycin (STR) was 32 µg/mL. At this concentration and above, the bacterial load decreased below the LLQ for CFUs (400 CFUs/mL) and MPNs (15 MPNs/mL) compared to untreated growth control levels (≈ 5×10^5 CFUs/mL and ≈ 8×10^6 MPNs/mL). The RS-ratio levels remained consistent with those of the untreated growth control (≈ 600–900) even at the highest concentration tested (128 µg/mL) (Fig. 3, **column 4**).

The MIC of LZD was established at 0.1875 µg/mL. Throughout the range of concentrations tested (from 192 µg/mL to 0.0117 µg/mL), a progressive decrease in bacterial load was observed for CFUs (from ≈ 5×10^5 to ≈ 3×10^3 CFUs/mL) and MPNs (from ≈ 2×10^6 to ≈ 6×10^3 MPNs/mL). The levels of rRNA exhibited a gradual decline (from ≈ 1×10^{11} to ≈ 1×10^9 copies/mL), although this occurred over a narrower concentration range (0.75 to 0.0117 µg/mL), remaining constant at concentrations ≥ 0.75 µg/mL, and the RS-ratio levels remained around untreated growth control values even at the highest concentrations tested, > 100 times the MIC (Fig. 3, **column 5**).

The MIC of INH was established at 0.03125 µg/mL. At the concentrations tested, the bacterial burden diminished from untreated growth control values to the LLQ of CFUs at concentrations higher than 0.5 µg/mL, while the LLQ of MPNs was observed at ≥ 8 µg/mL. The rRNA burden exhibited a marked reduction from untreated growth control values reaching approximately 1×10^9 copies/mL at concentrations ≥ 0.03125 µg/mL. The RS-ratio exhibited only a modest decline at concentrations ≥ 8 µg/mL and was reduced to ≈ 100 at 128 µg/mL, the maximum concentration tested (Fig. 4, **column 1**).

The MIC of EMB was established at 6 µg/mL. A progressive, dose-dependent reduction in bacterial burden was observed above the MIC concentrations, achieving a maximum reduction to the LLQ of CFUs and ≈ 1×10^3 MPNs/mL at 96 µg/mL, with a slight increase in burden at 384 µg/mL to ≈ 1×10^3 CFUs/mL and ≈ 5×10^3 MPNs/mL. The rRNA burden exhibited a maximal reduction to ≈ 1×10^9 copies/mL at concentrations ≥ 6 µg/mL. The RS-ratio remained unchanged when compared with the untreated growth control across the range of concentrations tested (Fig. 4, **column 2**).

The MIC of macozinone (also known as PBTZ169) was determined to be 0.0005 µg/mL. A progressive reduction in bacterial burden was observed across the range of concentrations tested (from 0.128 to 7.81×10^{-6} µg/mL) which appeared to reach a maximum decline to ≈ 3×10^4 MPNs/mL at ≥ 0.008 µg/mL, and ≈ 1×10^4 CFUs/mL at ≥ 0.0005 µg/mL. Notably, at two specific concentrations (0.128 and 0.008), no CFUs were detected, or they were below the LLQ. The rRNA burden declined to ≈ 1×10^9 copies/mL at ≥ 0.0005 µg/mL, while the RS-ratio remained unchanged across the concentrations tested (Fig. 4, **column 3**).

In the presence of clavulanic acid (CLV) at 5 µg/mL, the MIC of amoxicillin (AMX) was established at 2.5 µg/mL. The bacterial load decreased across the range of concentrations tested, reaching the LLQ of CFUs at ≥ 10 µg/mL, and the LLQ of MPNs at ≥ 160 µg/mL. The rRNA burden diminished progressively in a dose-dependent manner, achieving ≈ 3–5 × 10^7 copies/mL at ≥ 160 µg/mL. The RS-ratio values were not substantially reduced within the concentration range tested (640-0.039 µg/mL) (Fig. 4, **column 4**).

The MIC of pretomanid (PA-824) was determined to be 0.025 µg/mL. The bacterial burden progressively decreased at concentrations exceeding the MIC, until reaching the LLQ of CFUs at ≥ 1.6 µg/mL and a maximum reduction of ≈ 1×10^2 MPNs/mL at 6.4 µg/mL. The rRNA burden declined to ≈ 1×10^9 copies/mL at ≥ 0.025 µg/mL. PA-824 also promoted a progressive reduction of RS-ratio levels over MIC levels, decreasing to ≈ 20 at 6.4 µg/mL (Fig. 4, **column 5**).

Integrated analysis of biomarker relationships and drug-response profiles. The relationships among the different readouts were investigated using principal component analysis (PCA), with each observation corresponding to a single drug-concentration condition characterised by nine variables: resazurin conversion, CFUs, MPNs, 16S and 23S rRNA burden, and the four RS-ratio determinations. The first principal component accounted for 76.2% of the variance, while the second accounted for 19.4%. Together, the first two components explained 95.6% of the total variance, indicating that most of the variation in this fixed-endpoint dataset could be represented within a two-dimensional PCA space.

This can be better observed when projecting the nine variables onto the two principal component axes (Fig. 5a). There are two main groups of related readouts, one represented by REMA fluorescence (purple), CFUs and MPNs (black) and rRNA burdens (blue); whereas the four RS-ratios (green and red) appear consistently on a separate, nearly orthogonal axis. This separation into two blocks is also evident in the correlation matrix (Fig. 5b), where the four RS-ratios cluster together, and the remaining five variables form another coherent cluster. Both approaches indicate that the RS-ratio captures a component of the drug response that is not fully represented by growth inhibition, culturability, or total rRNA burden.

To examine the integrated response profiles of the different treatments, each drug-concentration condition was projected onto the two axes of the PCA. Increasing concentrations produced drug-specific trajectories that reflected the combined responses to all the biomarkers (Fig. 6a). Some conditions corresponding to drugs with related mechanisms of action (MoA) tended to occupy similar regions of the PCA space, although this organisation was not absolute and individual drugs retained distinct concentration-dependent profiles (Fig. 6b). This integrated analysis illustrated that the streamlined sample-preparation and inactivation workflow is compatible with the parallel determination of multiple molecular and culture-based readouts from the same

biological samples. The combined analysis provided a more comprehensive description of drug response than any individual readout alone, while reducing the need for separate samples or independent experiments for each biomarker.

Discussion

To support tuberculosis drug development, traditional readouts such as MIC, CFU, and MPN determinations remain essential. However, they do not directly capture the physiological state of *Mtb* following drug exposure. Molecular biomarkers based on rRNA can provide complementary information more rapidly: rRNA burden estimates bacterial load, whereas the RS-ratio reflects ongoing ribosomal biogenesis. Although these biomarkers have shown great promise in clinical samples and animal models, their implementation in early-stage, medium- to high-throughput *in vitro* drug and combination characterisation has not yet been reported, likely because conventional workflows require millilitre-scale sample volumes and separate analytical procedures. In this study, we addressed these constraints by reducing the required sampling volume to 50 µL and simultaneously determining both molecular biomarkers in a single-tube multiplexed ddPCR reaction. This miniaturised workflow enables a multidimensional characterisation of drug response directly from 96-well plate assays by integrating molecular biomarkers with conventional readouts obtained from the same biological samples.

We also established a preservation and inactivation workflow in which 50 µL of *Mtb* culture was mixed with 150 µL of DRSh and subjected to a validated heat treatment at either 80°C for 30 min or 99°C for 5 min. Both treatments achieved complete inactivation of high-burden *Mtb* cultures under the conditions tested. This procedure enables the transfer of inactivated samples outside BSL-3 facilities for downstream RNA extraction and molecular biomarker analysis in appropriately authorised laboratories.

The multiplexed approach enabled the simultaneous determination of two complementary molecular biomarkers: total rRNA burden and ongoing ribosomal biogenesis, estimated using the RS-ratio. Moreover, the pentaplex ddPCR reaction allowed us to evaluate how target selection influenced both biomarker determinations. Quantification of rRNA burden using either 23S or 16S rRNA yielded highly similar treatment-response profiles, consistent with previous observations in clinical samples [11]. Likewise, the different target pairs used to calculate the RS-ratio generally produced comparable profiles across drugs and concentrations, although RMP revealed notable differences, as discussed below. Among the four combinations, ETS1/23S exhibited the widest dynamic range, whereas ITS1/16S showed the narrowest. The PCA and correlation analyses support simplification of the molecular assay by showing substantial redundancy between the two total-rRNA targets and among the four RS-ratio combinations (Fig. 5). These analyses do not determine which specific targets should be retained, but given the superior dynamic range of the ETS1/23S pair and the highly similar treatment-response profiles obtained with 16S and 23S rRNA, future molecular assays can be streamlined by targeting only ETS1, 23S rRNA, and the spiked EC.

Although the proof-of-concept drug characterisation was performed using the *Mtb* H37Ra strain, the results illustrate the complementary information provided by the different conventional readouts. In this experiment, MICs generally occurred at concentrations associated with bacterial loads below ≈ 5×10^4 CFUs/mL or 2×10^5 MPNs/mL and rRNA burdens below ≈ 5×10^9 copies/mL. In the optimised CFU and MPN workflow developed within the ERA4TB consortium, the MPN assay provided a LLQ of approximately 15 MPNs/mL, compared with 400 CFUs/mL. MPN measurements were generally 0.5–1.5 $\log_{10}$ higher than CFU counts, highlighting their contribution to the recovery of differentially culturable bacilli. Furthermore, adding activated charcoal to the MPN broth reduced the effect of antibiotic carry-over and improved bacterial recovery at high drug concentrations, including selected conditions exceeding 100 times the MIC. In the absence of activated charcoal, lower MPN estimates or no detectable growth were observed at some high drug concentrations, particularly for RMP (**Supplementary Figure S2**).

At supra-inhibitory concentrations, rRNA burden frequently reached a plateau of ≈ $3–6 \times 10^8$ copies/mL, except with AMX + CLV, despite substantial differences in CFU and MPN measurements. For example, at the highest LZD and BDQ concentrations, ≈ 10^4 growth units/mL remained detectable, whereas STR and INH reduced both CFUs and MPNs below their respective LLQ; nevertheless, the corresponding rRNA burdens were similar (Figs. 3 and 4). This decoupling may have two non-exclusive explanations. First, rRNA burden may include signals from bacilli that remain viable but are not recovered by CFU or MPN. Second, rRNA may persist after loss of culturability or bacterial death and therefore decline more slowly than culture-based readouts. Because rRNA extraction provides a population-averaged measurement, the present data cannot distinguish between these possibilities.

Our results are more consistent with substantial persistence of rRNA after loss of culturability, as most of the drugs tested do not directly disrupt the bacterial cell envelope and intact cellular structures may delay RNA degradation. In a preliminary TKA, rRNA burden remained close to the day-0 inoculum level after 14 days of RMP exposure, whereas CFUs declined to fewer than 20 CFUs/mL (**Supplementary Figure S3**). A similar discrepancy has been reported in BALB/c mice, where potent regimens produced an approximately 6 $\log_{10}$ reduction in CFUs after four weeks of treatment but less than a 2 $\log_{10}$ reduction in 16S rRNA burden [8]. AMX + CLV was an exception in the present experiment, reducing rRNA burden to ≈ $3–5 \times 10^7$ copies/mL. One possible explanation is that cell-wall damage and lysis induced by AMX + CLV facilitate the release and subsequent degradation of bacterial rRNA, although this mechanism was not directly assessed.

The RS-ratio showed drug- and concentration-dependent behaviour that appeared to be associated with drug MoA. The strong reduction induced by RMP is readily explained by its direct inhibition of RNA polymerase activity [12–14]. Because no resazurin conversion occurred across the full concentration range tested, the experiment did not yield a reliable MIC-centred concentration-response profile for RMP and may have been affected by an experiment-specific technical limitation. The RMP results should therefore be interpreted primarily as a mechanistically informative reference for RNA-polymerase inhibition and RS-ratio behaviour, rather than as a complete pharmacodynamic characterisation of RMP potency. Nevertheless, residual culturable bacteria remained detectable, and the RS-ratio showed a modest concentration-response: the lowest concentration tested, 0.78 ng/mL, producing a smaller reduction than higher concentrations, in agreement with previous observations in *Mtb* [9, 15]. RMP was also the only drug for which the magnitude of the response differed markedly among the four RS-ratio target pairs. We recently observed a similar pattern in *M. ulcerans* TKAs treated with RMP alone or in combination with clarithromycin and/or AMX + CLV [16]. The reproducibility of this pattern across mycobacterial species suggests that it is unlikely to be solely an assay

artefact and may reflect the combined effects of direct pre-rRNA transcriptional inhibition and different degradation kinetics of ETS1 and ITS1 during rRNA processing. Further studies with other rifamycins and transcription inhibitors will be required to determine whether this represents a broader signature of RNA-polymerase inhibition.

MXF reduced the RS-ratio above its MIC, although less markedly than RMP, in agreement with previous observations [15]. Unlike the other drugs that reduced the RS-ratio, MXF showed a non-monotonic concentration-response pattern: the strongest reduction occurred at an intermediate concentration, followed by a partial recovery at higher concentrations. Fluoroquinolone-mediated DNA damage is known to activate the SOS response in *Mtb*, and MXF also induces redox stress and broader transcriptional adaptations [17, 18]. These responses could alter transcriptional regulation and rRNA biogenesis, and potentially contribute to the non-monotonic RS-ratio profile observed here. However, SOS-response markers were not measured, and the experiment was performed at a single endpoint; therefore, the present data cannot directly attribute this pattern to SOS activation. Further temporal and mechanistic studies would be required to test this hypothesis.

BDQ induced a concentration-dependent reduction in the RS-ratio, consistent with previous reports [9, 15]. Because rRNA biogenesis is energetically demanding, this response is compatible with the inhibition of ATP synthesis caused by BDQ [19]. This pattern contrasts with protein-synthesis inhibitors and most cell-wall-targeting drugs, as discussed below, supporting the interpretation that the RS-ratio captures physiological constraints on ribosomal biogenesis rather than simply reflecting loss of culturability or total bacterial burden. However, ATP levels and respiratory activity were not measured here, so this mechanistic interpretation remains indirect.

The protein-synthesis inhibitors STR and LZD had little or no effect on the RS-ratio. Even when STR reduced CFUs and MPNs below their limits of quantification, the RS-ratio remained close to growth-control levels. Previous studies similarly found that STR [9] and LZD [15] did not reduce the RS-ratio and could produce modest increases. A comparable increase was observed in *M. ulcerans* exposed to clarithromycin [16]. These increases could reflect a compensatory response to ribosomal inhibition, involving continued or increased production of precursor ribosomal components; however, the regulatory mechanisms underlying this response were not investigated here.

Drugs targeting different stages of cell-wall biosynthesis generally produced little or no reduction in the RS-ratio. EMB, as previously reported [9, 15], did not substantially alter the ratio, and similar behaviour was observed with PBTZ169 and AMX + CLV. To our knowledge, these are the first observations of this response for PBTZ169 and AMX + CLV in *Mtb*, although a comparable result was reported for AMX + CLV in *M. ulcerans* [16]. INH produced only a modest RS-ratio reduction, consistent with previous reports [9, 15], and only at concentrations of at least 8 µg/mL, corresponding to 256 times its MIC. This response was decoupled from the other biomarkers and occurred at higher concentrations than the marked reductions in CFUs, MPNs, and rRNA burden. Consequently, the INH-associated RS-ratio reduction should be interpreted cautiously and may have limited pharmacodynamic relevance.

In contrast, PA-824 produced a marked RS-ratio reduction, consistent with previous reports [15], that was accompanied by reductions in bacterial load and rRNA burden. This response should not be interpreted solely as a consequence of cell-wall inhibition, because PA-824 has a multifaceted MoA that includes inhibition of mycolic-acid biosynthesis and the induction of respiratory and nitrosative stress [20]. These additional effects may contribute to its stronger and more coherent impact on ribosomal biogenesis.

Taken together, these findings indicate that the RS-ratio is not simply a surrogate for bacterial culturability or total bacterial burden, but a complementary biomarker reflecting changes in ongoing ribosomal biogenesis. This interpretation is supported by the PCA and correlation analyses, in which the RS-ratio measurements formed a separate cluster from resazurin conversion, CFUs, MPNs, and rRNA burden. More broadly, MIC, CFU, MPN, rRNA burden, and RS-ratio should not be considered interchangeable readouts, as each captures a different component of drug response. Murine studies have shown that combining RS-ratio and CFU can improve discrimination between drug treatments [8]. Additional murine and clinical studies have demonstrated that the RS-ratio provides information distinct from burden-based readouts [9, 11, 21]. Incorporating this complementary approach into *in vitro* assays may therefore provide a richer pharmacodynamic description from the earliest stages of drug and combination evaluation and facilitate subsequent integration with preclinical and clinical data.

Our results also indicate that the performance and interpretation of molecular biomarkers depend on the experimental and biological context. In this fixed 6-day *in vitro* proof-of-concept, rRNA burden showed limited additional dynamic range once culturable bacterial counts fell below a certain threshold. This plateau may reflect slow degradation or persistence of rRNA after loss of culturability and may limit the ability of rRNA burden to discriminate among highly bactericidal conditions in fixed-endpoint *in vitro* assays [8]. However, this observation does not diminish its potential value in other settings. In clinical studies, rRNA burden is measured longitudinally and has been successfully used to monitor progressive changes in sputum bacterial load during treatment [6, 7, 22, 23].

Although the temporal dimension is important for all biomarkers, it may be particularly informative for interpreting the RS-ratio. The absence of an RS-ratio reduction does not necessarily indicate a lack of drug activity, because CFUs and MPNs may decline without a parallel change in ribosomal biogenesis. Conversely, an initial reduction followed by a later increase could indicate renewed pre-rRNA synthesis and recovery of ribosomal biogenesis. However, such an increase cannot by itself demonstrate bacterial regrowth, persistence, or resistance, which would require supporting culture-based, phenotypic, or genetic evidence. This hypothesis is consistent with our previous observations in *M. ulcerans*, where the RS-ratio increased at later treatment time points despite no detectable regrowth in the retrospective experiment [16], and with murine observations showing that the RS-ratio increased more rapidly than CFUs after treatment withdrawal [24]. These findings support further longitudinal evaluation of the RS-ratio as an early marker of physiological recovery.

Importantly, this study was not designed to provide definitive pharmacodynamic profiles of the individual drugs tested, but rather as a proof-of-concept for the integration of molecular and culture-based biomarkers into medium- to high-throughput *in vitro* workflows. The principal contribution of the platform is operational: it enables multidimensional biomarker evaluation from the same biological samples in 96-well formats [4], together with validated sample

preservation, inactivation, and transfer outside BSL-3 facilities. This platform could therefore support future drug-combination evaluations within initiatives such as ERA4TB. The workflow could also be adapted to lower-throughput but more physiologically relevant settings, provided that each application is validated in its specific matrix and context.

This proof-of-concept has several limitations. It was performed using the *Mtb* H37Ra strain, under a single set of *in vitro* conditions, and primarily at a fixed 6-day endpoint. The concentration ranges were not optimised to provide complete pharmacodynamic profiles for every compound, and no systematic drug-combinations were tested here. Differences from results obtained in more physiological models may reflect strain background, medium composition, drug concentration range, or treatment duration. Although the workflow is compatible with 96-well sampling and downstream ddPCR determination, mechanical lysis remains a practical throughput bottleneck.

A further limitation is that RNA extraction and ddPCR provide a population-averaged molecular signal and cannot resolve phenotypically distinct bacterial subpopulations. FISH and microscopy have identified spatially separated *Mtb* populations with different RS-ratio levels in the cellular rim and caseum of C3HeB/FeJ mouse granulomas [9], findings subsequently supported by RNA analysis of microdissected samples [25]. If subpopulations with different drug responses are present in the *in vitro* assays, their signals may be obscured by the dominant population. Single-cell or spatially resolved approaches could help identify such heterogeneity, although they are not currently readily compatible with medium- to high-throughput drug evaluation.

Overall, we present a practical platform compatible with medium- to high-throughput evaluation of antitubercular drug responses and future combination studies, integrating conventional culture-based readouts with two molecular biomarkers: rRNA burden and RS-ratio. Their incorporation enables a more multidimensional characterisation of drug response from the early stages of preclinical evaluation. Rather than replacing conventional readouts, the platform expands the information obtained from the same biological samples and may strengthen the connection between *in vitro* drug characterisation and subsequent preclinical and clinical studies.

Methods

Drug characterisation and preparation. Pre-inocula of *Mtb* H37Ra were cultured at 37°C in Middlebrook 7H9 broth (Difco) supplemented with 0.025% tyloxapol, 0.2% glycerol, and 10% (v/v) oleic acid-albumin-dextrose-catalase (OADC, Middlebrook) until reaching mid-exponential phase. 96-well plates were inoculated with 250 µL of broth containing approximately 10^5 CFU/mL. The different antibiotics were added by dispensing 2.5 µL of 100 × working solutions prepared in the appropriate solvents (see Table 1 for details). After incubation for 6 days at 37°C, samples were processed for multiple endpoints: 20 µL were collected for MPN and CFU determination, 50 µL were collected for molecular biomarker determination, and the remaining volume was used for MIC assessment. For the preliminary TKA with INH and RMP, a single flask was used per condition. The drugs were added at 10 and 1 µg/mL, respectively, in broth, and 50 µL were collected for molecular biomarker determinations and 50 µL for CFU determination at days 0, 2, 6, 14, and 20 post-exposure.

Table 1
Specifications of the drugs used in this study.

Abbr.	Drug	Range tested (µg/mL)	
EMB	Ethambutol	384	0.0234
RMP	Rifampicin	12.8	7.81E-04
INH	Isoniazid	128	0.0078
STR	Streptomycin	128	0.0078
MXF	Moxifloxacin-sulfate	6.4	0.0004
LZD	Linezolid	192	0.0117
AMX	Amoxicillin	640	0.0391
CLV	Clavulanate	5	
PA-824	Pretomanid	25.6	0.0016
BDQ	Bedaquiline	6.4	0.0004
PBTZ169	Macozinone	0.128	7.81E-06

Viability determination. MICs were determined after six days of incubation of *Mtb* H37Ra cultures with the compounds. 30 µL of 0.1 mg/mL filter-sterilised resazurin (Sigma-Aldrich) were added to ≈ 180 µL of broth in each well. Plates were incubated for 16 h at 37°C. The MIC was determined as the lowest concentration at which no colour change was observed. Fluorescence was recorded using a Biotek Synergy HT system, using the corresponding excitation (530/25) and emission (590/35) filters. CFU and MPN were determined using protocols adapted from those previously described by Rabodoarivelo and colleagues [4]. Briefly, 20 µL were collected from each condition and transferred to the first row of 96-well plates, with 180 µL of 7H9 broth-OADC and 0.4% (w/v) activated charcoal in each well. Serial 10-fold dilutions were done in the remaining rows. From each dilution, 2.5 µL were plated onto solid Middlebrook 7H10 agar supplemented with 0.2% glycerol, 10% OADC, and activated charcoal 0.4 % w/v). For CFU determination, 7H10 agar plates were incubated at 37°C for 21 days. Colonies were counted, and bacterial load was expressed as CFU/mL. CFU values were summarised as geometric means across the available countable replicate wells, with geometric standard deviations used to describe variability. For MPN determination, 7H9 broth plates were incubated at 37°C for 28 days. The number of wells showing visible turbidity at each dilution was recorded and confirmed by the addition of 30 µL of 0.1 mg/mL filter-sterilised

resazurin. The bacterial load and confidence intervals (MPNs/mL) were calculated using the recommended guidelines [26]. MPN values are reported with their 95% confidence intervals. Up to three replicate wells were available per condition.

Quantification of the molecular biomarkers rRNA burden and synthesis ratio using droplet digital PCR. To assess molecular biomarkers of *Mtb*, 50 µL of each sample was mixed with 150 µL of DNA/RNA Shield (Zymo, R1100-250) spiked with ≈ 10^8 copies of *Solanum tuberosum* (*phyB* gene) mRNA *in vitro* synthesised as previously described [7]. This mRNA was used as an EC RNA for the extraction process. Samples were heat-inactivated at 80°C for 30 min and stored at – 80°C until RNA extraction. For RNA extraction, 200 µL of thawed samples were added to 500 µL of TriReagent (Zymo, R2050-1200) and homogenised in 2 mL tubes containing 0.1 mm zirconia beads (BeadBug™ Z763764-50EA) using a FastPrep-24 5G (MP Biomedicals). Extraction was completed following the DirectZol 96 RNA kit protocol (Zymo, R2056) using 400 µL of the lysate supernatant. RNA was eluted in 25 µL of RNase/DNase-free water. Reverse transcription was performed with SUPERSCRIPT IV VILO MasterMix (Thermo Fisher, Ref. 11756500) in a final volume of 10 µL using 5 µL of RNA. The reaction was incubated at 25°C for 10 min and 50°C for 15 min. Quantification of the targets was performed in multiplex reactions using ddPCR SuperMix for Probes (no dUTP) (Bio-Rad). Primers were used at 900 nM and probes at 250 nM (Bio-Rad or CertTest S.L.). Primer and probe sequences were previously published [7, 9]. After droplet generation, thermal cycling conditions were: 95°C for 10 min; 40 cycles of 96°C for 45 s and 60°C for 105 s (2°C/s ramp rate); and a final hold at 98°C for 10 min. The number of copies for each target, ETS1 (FAM), 23S rRNA (HEX), 16S rRNA (Cy5), ITS1 (FAM or ROX), and EC RNA (Cy5.5) were quantified from the partitioned droplets using the QX600 Droplet Digital PCR System (Bio-Rad) and the QX Manager Standard Edition v2.4.0.70 (Bio-Rad). The RS-ratio was calculated as the ratio of the copy number of the precursor rRNA (ETS1 or ITS1) to the copy number of the total rRNA (23S or 16S), multiplied by 10^4, as previously described [9]. The rRNA burden was calculated by dividing the copy number of total rRNA (23S or 16S) by the copy number of EC RNA, multiplied by a 2×10^9 copies/mL factor (≈ 10^8 copies EC RNA mixed with 0.05 mL of sample), and values were expressed as copies/mL. For each condition, rRNA burden and RS-ratio values were summarised as geometric means across the available quantifiable replicate wells, with geometric standard deviations used to describe variability. Up to three replicate wells were available per condition.

Mathematical analysis. For each drug-concentration, nine quantitative variables were included in the multivariate analysis: REMA fluorescence, CFUs, MPNs, two rRNA burden determinations based on 16S and 23S rRNA, and four RS-ratio determinations derived from the combinations of ETS1 or ITS1 with 16S or 23S rRNA. A matrix was constructed from all nine-component vectors (eight per drug, all drugs together), and principal component analysis (PCA) was performed on this data set in order to understand its underlying dimensionality. Prior to PCA, log10-transformed values were standardised to account for differences in scale between variables. Pairwise Pearson correlation coefficients were also calculated to assess relationships between readouts.

Use of AI-assisted tools. OpenAI language models were used for editorial assistance with the harmonization of text and the correction of grammatical and stylistic errors. Authors are solely responsible for the accurate content of this work.

Declarations

Funding:

The project leading to this publication has received funding from the Innovative Medicines Initiative 2 Joint Undertaking (JU) under grant agreement No 853989 (https://era4tb.org/) to JJV. The JU receives support from the European Union's Horizon 2020 Research and Innovation Programme and EFPIA and Global Alliance for TB Drug Development Non-Profit Organisation, Bill & Melinda Gates Foundation, University of Dundee. PCF acknowledges support from grants PID2022-142185NB-C22 and PID2025-171290NB-C22 funded by MCIN/AEI/10.13039/501100011033 and by "ERDF: A way of making Europe." This work reflects only the author's views, and the JU is not responsible for any use that may be made of the information it contains.

Author Contribution

Conceptualization: JCS, SFB, AML. Data curation: JCS, LTH, LYF. Formal analysis: JCS, LYF, PCF. Funding and project administration: JJV. Investigation: JCS, LTH, FDA. Methodology: JCS. Supervision: SFB, AML. Visualization: JCS, PLE, LYF, PCF. Original draft writing: JCS. Writing – review & editing: All authors.

Acknowledgement

We would like to acknowledge the technical staff of the CleanRooms of the Bioengineering facility core of Universidad Carlos III de Madrid, which housed our experimental activities.

Data Availability

The datasets generated during and/or analysed during the current study are available from the corresponding author upon reasonable request.

Code availability

The Python code used for principal component analysis and Pearson correlation analysis (Figs. 5 and 6) is available from the corresponding author upon reasonable request.

References

1. Paulson, T. & Epidemiology A mortal foe. *Nature* **502**, 2–S3 (2013).
2. WHO. *Global Tuberculosis Report 2025*. (2025). https://www.who.int/teams/global-programme-on-tuberculosis-and-lung-health/tb-reports/global-tuberculosis-report-2025
3. European Regimen Accelerator for Tuberculosis. (ERA4TB). https://era4tb.org/
4. Rabodoarivelo, M. S. et al. Protocol to quantify bacterial burden in time-kill assays using colony-forming units and most probable number readouts for Mycobacterium tuberculosis. *STAR. Protoc.* **6**, 103643 (2025).
5. Arenaz-Callao, M. P. et al. OPTIKA, a new high content kill-kinetic assay to longitudinally assess *in vitro* drug combinations against *Mycobacterium tuberculosis*. Preprint at (2026). https://doi.org/10.64898/2026.05.10.724062
6. Sabiiti, W. et al. A Tuberculosis Molecular Bacterial Load Assay (TB-MBLA). *J. Visualized Experiments*. **e60460** 10.3791/60460 (2020).
7. Honeyborne, I. et al. Molecular Bacterial Load Assay, a Culture-Free Biomarker for Rapid and Accurate Quantification of Sputum Mycobacterium tuberculosis Bacillary Load during Treatment. *J. Clin. Microbiol.* **49**, 3905–3911 (2011).
8. Dide-Agossou, C. et al. Combination of Mycobacterium tuberculosis RS Ratio and CFU Improves the Ability of Murine Efficacy Experiments to Distinguish between Drug Treatments. *Antimicrob. Agents Chemother.* **66**, e0231021 (2022).
9. Walter, N. D. et al. Mycobacterium tuberculosis precursor rRNA as a measure of treatment-shortening activity of drugs and regimens. *Nat. Commun.* **12**, 2899 (2021).
10. Krausser, L. et al. Mycobacterium tuberculosis retains viability in RNAlater buffer but not in GTC-TCEP and DNA/RNA Shield. *Diagn. Microbiol. Infect. Dis.* **106**, 115905 (2023).
11. Musisi, E. et al. Reproducibility of the Ribosomal RNA Synthesis Ratio in Sputum and Association with Markers of Mycobacterium tuberculosis Burden. *Microbiol. Spectr.* **9**, e0048121 (2021).
12. Konno, K., Oizumi, K. & Oka, S. Mode of action of rifampin on mycobacteria. II. Biosynthetic studies on the inhibition of ribonucleic acid polymerase of Mycobacterium bovis BCG by rifampin and uptake of rifampin- 14 C by Mycobacterium phlei. *Am. Rev. Respir Dis.* **107**, 1006–1012 (1973).
13. White, R. J., Lancini, G. C. & Silvestri, L. G. Mechanism of Action of Rifampin on *Mycobacterium smegmatis*. *J. Bacteriol.* **108**, 737–741 (1971).
14. Honore, N. & Cole, S. T. Molecular basis of rifampin resistance in Mycobacterium leprae. *Antimicrob. Agents Chemother.* **37**, 414–418 (1993).
15. Reichlen, M. J. et al. Standardized RS Ratio Metrics To Assess Tuberculosis Antimicrobial Efficacy and Potency. *Antimicrob. Agents Chemother.* **67**, e0148322 (2023).
16. Calvet-Seral, J. et al. The ribosomal RNA synthesis ratio biomarker in Mycobacterium ulcerans for drug activity evaluation. *Infect. Dis. Poverty*. **15**, 51 (2026).
17. Iacobino, A., Piccaro, G., Pardini, M., Fattorini, L. & Giannoni, F. Moxifloxacin Activates the SOS Response in Mycobacterium tuberculosis in a Dose- and Time-Dependent Manner. *Microorganisms* **9**, 255 (2021).
18. Shee, S. et al. Moxifloxacin-Mediated Killing of Mycobacterium tuberculosis Involves Respiratory Downshift, Reductive Stress, and Accumulation of Reactive Oxygen Species. *Antimicrob. Agents Chemother.* **66**, e0059222 (2022).
19. Andries, K. et al. A diarylquinoline drug active on the ATP synthase of Mycobacterium tuberculosis. *Science* **307**, 223–227 (2005).
20. Baptista, R., Fazakerley, D. M., Beckmann, M., Baillie, L. & Mur, L. A. J. Untargeted metabolomics reveals a new mode of action of pretomanid (PA-824). *Sci. Rep.* **8**, 5084 (2018).
21. Sordello, S. et al. A modeling-based framework to evaluate forgiveness of tuberculosis treatment in a BALB/c relapsing mouse model. *Antimicrob. Agents Chemother.* **70**, e01109–e01125 (2026).
22. Honeyborne, I. et al. The Molecular Bacterial Load Assay Replaces Solid Culture for Measuring Early Bactericidal Response to Antituberculosis Treatment. *J. Clin. Microbiol.* **52**, 3064–3067 (2014).
23. Honeyborne, I. et al. Profiling persistent tubercule bacilli from patient sputa during therapy predicts early drug efficacy. *BMC Med.* **14**, 68 (2016).
24. Hendrix, J. et al. Physiologic recovery of Mycobacterium tuberculosis from drug injury: A molecular study of post antibiotic effect in vitro and in vivo. *PLoS Pathog*. **22**, e1014131 (2026).
25. Walter, N. D. et al. Lung microenvironments harbor *Mycobacterium tuberculosis* phenotypes with distinct treatment responses. *Antimicrob. Agents Chemother.* **67**, e00284–e00223 (2023).
26. Bacteriological Analytical Manual Appendix 2. Most Probable Number from Serial Dilutions. (2023). https://www.fda.gov/food/laboratory-methods-food/bam-appendix-2-most-probable-number-serial-dilutions

Figures

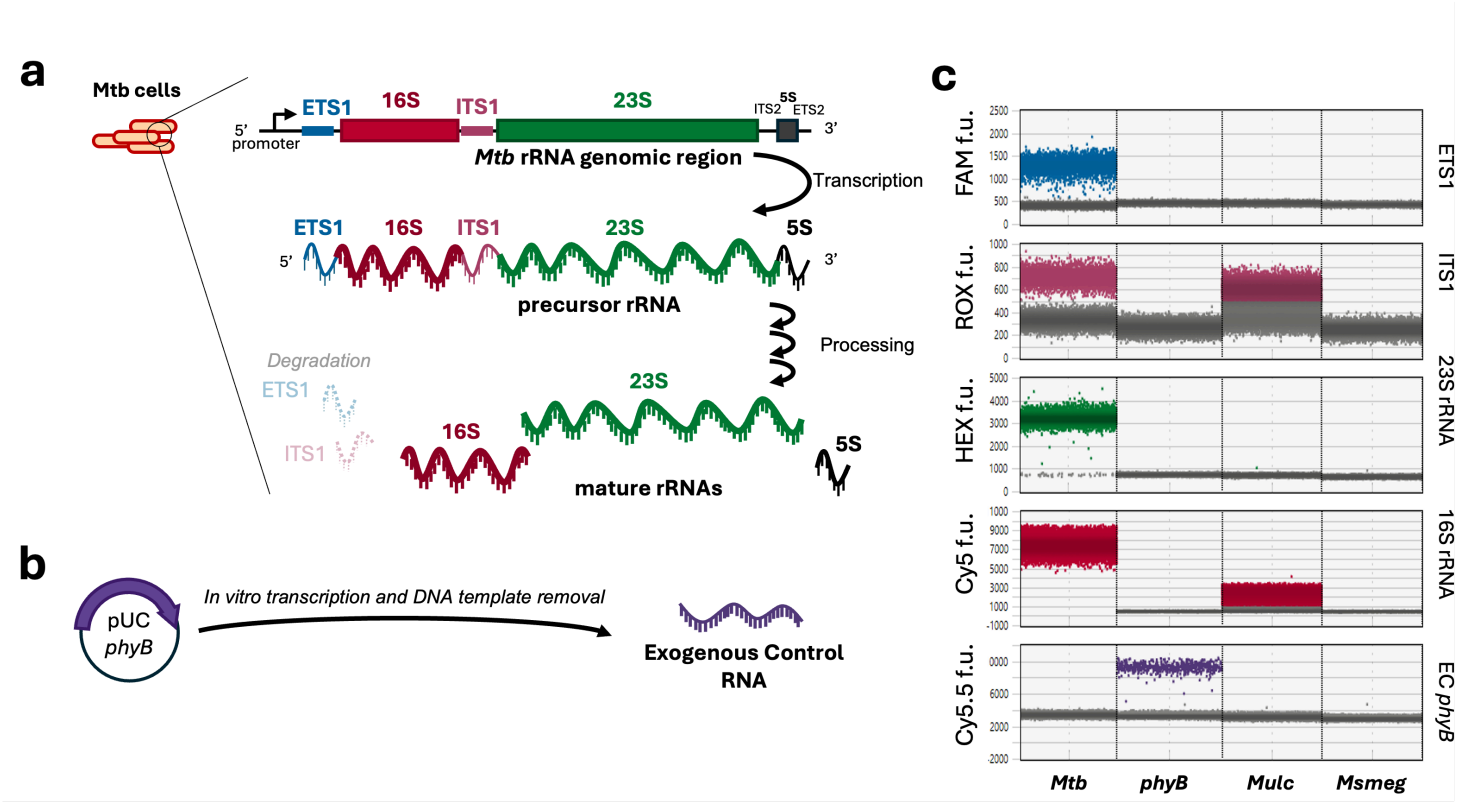

Figure 1

Design and specificity of the multiplexed ddPCR assay. a) The *Mtb* rRNA genomic region encodes the different bacterial targets used for the rRNA burden and RS-ratio determination: ETS1, 16S rRNA, ITS1, and 23S rRNA (ITS2, 5S rRNA, and ETS2 were not included in this study). After transcription, the first rRNA molecule (precursor rRNA) contains all the regions, but through rRNA maturation and processing, ETS1 and ITS1 are degraded, and mature rRNAs are the ones remaining. **b)**The *phyB* gene of *S. tuberosum* was chemically synthesised downstream of the T7 promoter, and the EC RNA was obtained by in vitro transcription and subsequent DNA digestion and RNA isolation. **c)** Droplet amplitude results of the multiplexed ddPCR for ETS1 (FAM), ITS1 (ROX), 23S rRNA (HEX), 16S rRNA (Cy5), and EC (Cy5.5) with different templates. The primers and probe sets used for the detection of the EC or the different *Mtb* rRNA targets were tested against *Mtb*, *S. tuberosum phyB*, *M. ulcerans* and *M. smegmatis* genetic material.

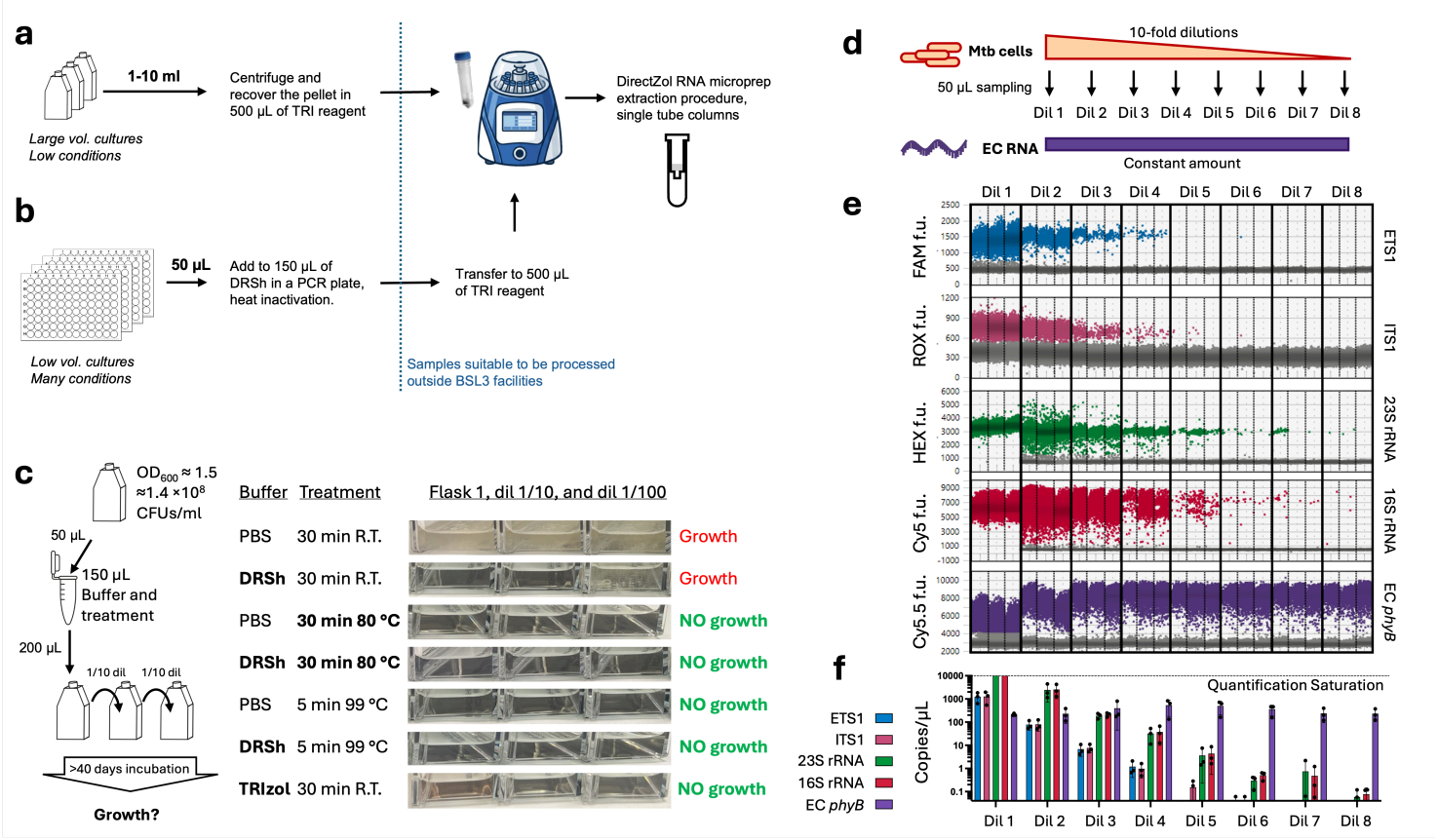

Figure 2

Miniaturised RNA workflow, sample inactivation, and assay performance across bacterial dilutions. a) Schematic representation of the conventional workflow using large-volume sampling versus **b)** the proposed small-volume sampling for increasing the compatibility of RNA extraction from large *Mtb in vitro* drug characterisations. **c)** Inactivation test of high-burden *Mtb in vitro* samples comparing saline buffer PBS, DRSh, Trizol, and incubating for 30 min at 80 °C or 5 min at 99 °C. **d)**Schematic representation of a burden curve of *Mtb* for RNA extraction with constant amounts of EC RNA. **e)** Droplet amplitude results of the multiplexed ddPCR for ETS1 (FAM), ITS1 (ROX), 23S rRNA (HEX), 16S rRNA (Cy5), and EC (Cy5.5). **f)** Quantification of the different targets reported by the QX Manager software. The dots represent individual well values, and columns and error bars represent the mean and standard deviation, respectively.

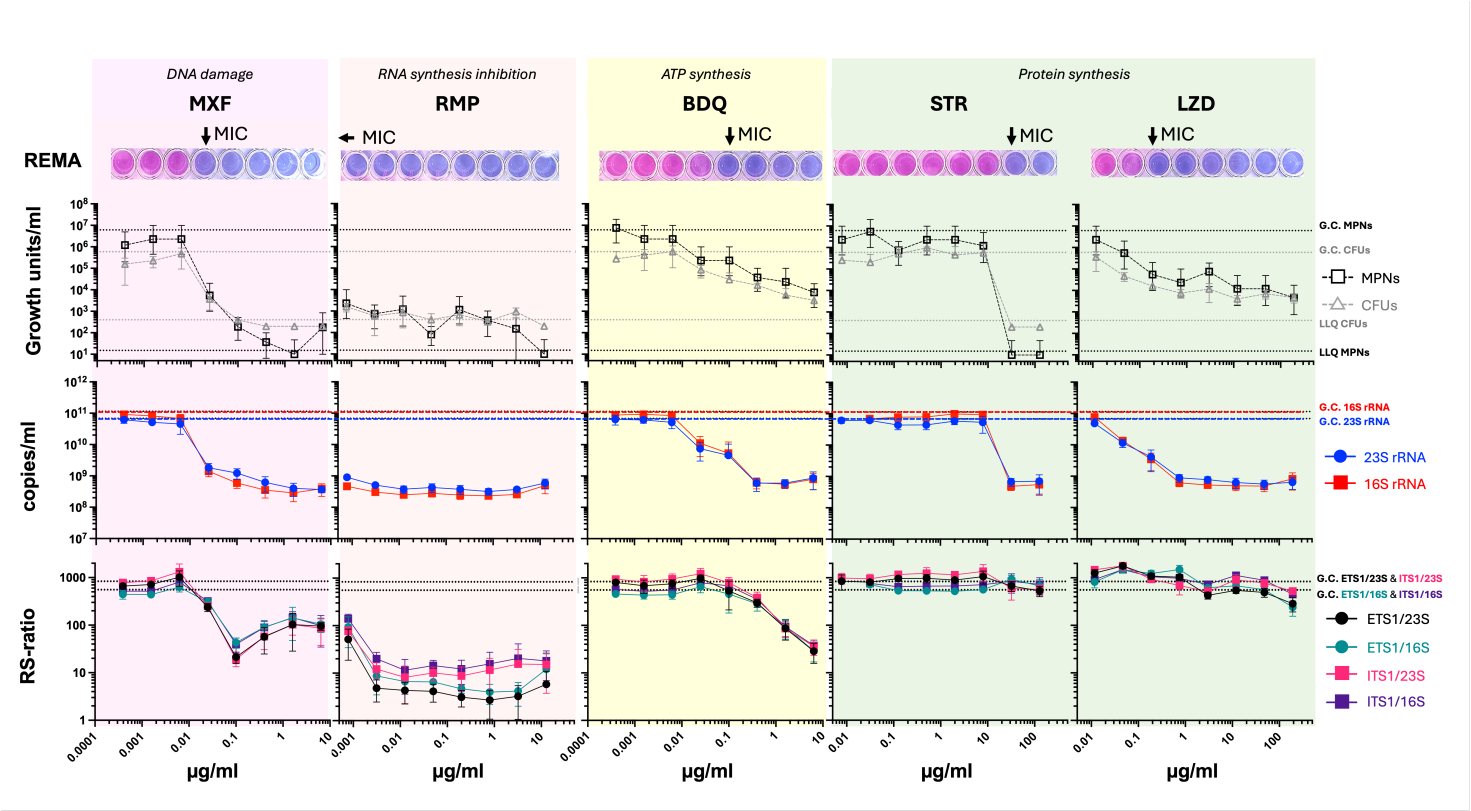

Figure 3

Drug-response profiles for moxifloxacin, rifampicin, bedaquiline, streptomycin, and linezolid. Three replicates of *Mtb* H37Ra were incubated with different concentrations of moxifloxacin (MXF, column 1), rifampicin (RMP, column 2), bedaquiline (BDQ, column 3), streptomycin (STR, column 4), and linezolid (LZD, column 5). Results of resazurin conversion (row 1), growth units/mL measured by colony-forming units (CFUs, grey empty triangles) or most probable number (MPNs, black empty squares) (row 2), 16S (red squares) and 23S (blue circles) rRNA burden (row 3), and the RS-ratio results using the four different possible pairs (row 4). Graphs are highlighted depending on their mode of action: DNA damage (pink), RNA synthesis inhibition (red), ATP synthesis inhibition (yellow), and protein synthesis inhibition (green). For CFU, rRNA burden, and RS-ratio, values are shown as geometric means of the available replicate wells, with error bars representing geometric standard deviations when more than one value was available. Up to three replicate values were available per condition. MPN values are shown with their corresponding 95% confidence intervals.

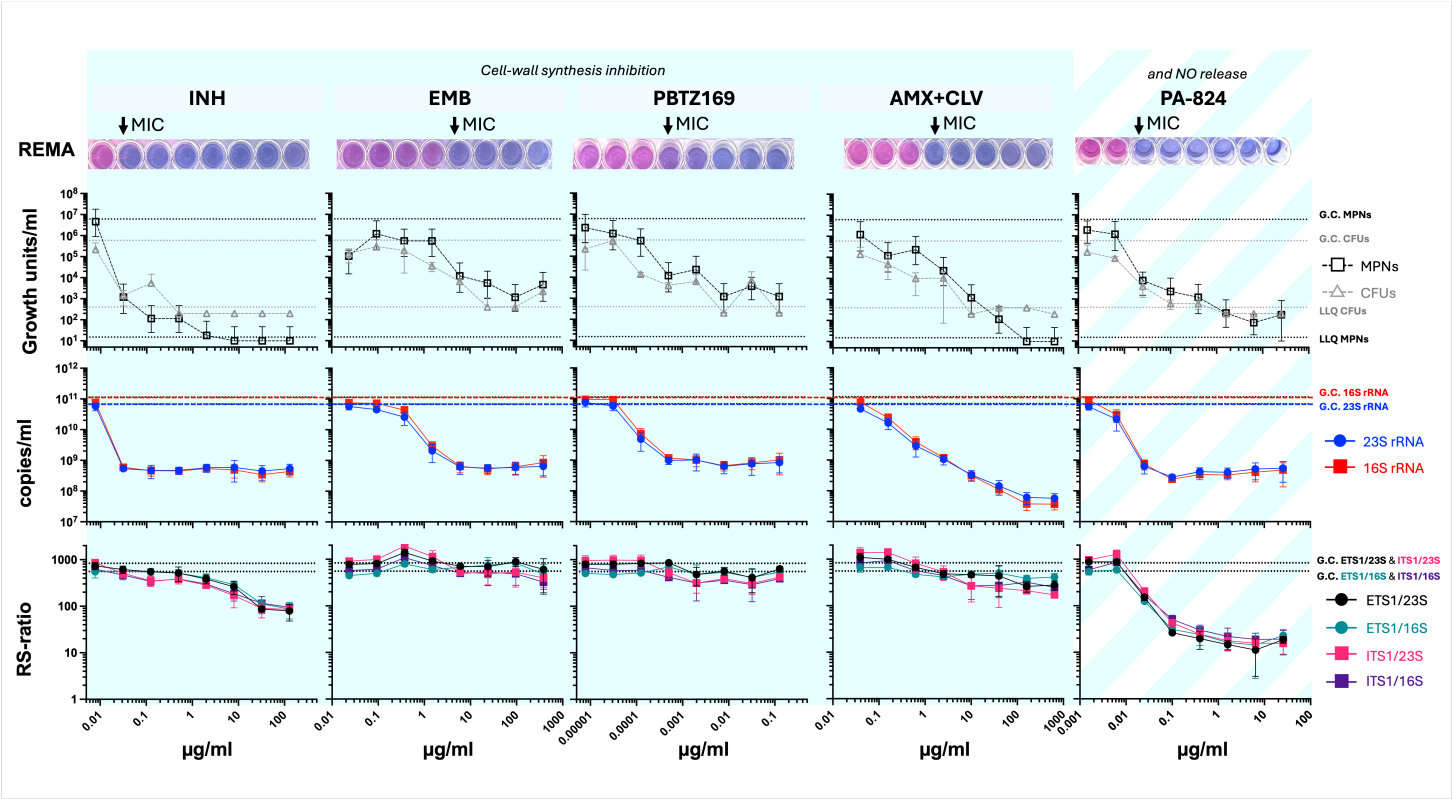

Figure 4

Drug-response profiles for isoniazid, ethambutol, macozinone, amoxicillin-clavulanate, and pretomanid. Three replicates of *Mtb* H37Ra were incubated with different concentrations of isoniazid (INH, column 1), ethambutol (EMB, column 2), macozinone (PBTZ169, column 3), amoxicillin-clavulanate (AMX+CLV, column 4), and pretomanid (PA-824, column 5). Results of resazurin conversion (row 1), growth units/mL measured by colony-forming units (CFUs, grey empty triangles) or most probable number (MPNs, black empty squares) (row 2), 16S (red squares) and 23S (blue circles) rRNA burden (row 3), and the RS-ratio results using the four different possible pairs (row 4). Graphs are highlighted depending on their mode of action: cell-wall synthesis inhibition (pale blue) and NO release (white). For CFU, rRNA burden, and RS-ratio, values are shown as geometric means of the available replicate wells, with error bars representing geometric standard deviations when more than one value was available. Up to three replicate values were available per condition. MPN values are shown with their corresponding 95% confidence intervals.

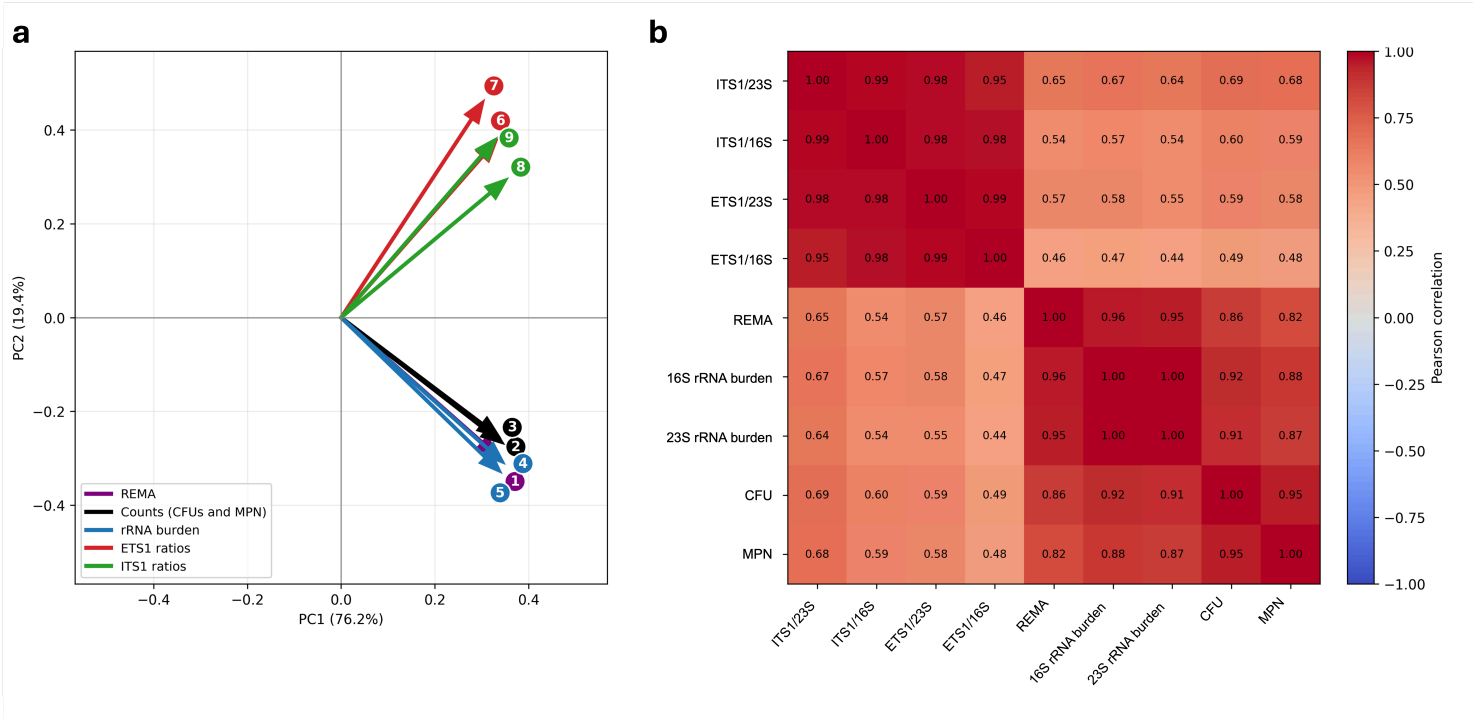

Figure 5

Relationships among molecular, phenotypic, and culture-based readouts. a) Projection of the nine measured readouts onto the first two principal components. The variables include resazurin conversion (purple), CFUs and MPNs (black), rRNA burdens (blue), and the four RS-ratios (green and red). The first and second principal components explain 76.2% and 19.4% of the total variance, respectively. **b)** Correlation matrix of the nine biomarker readouts across the drug-concentration conditions. The four RS-ratios form a related cluster that is distinct from the growth-, culturability-, and burden-associated readouts.

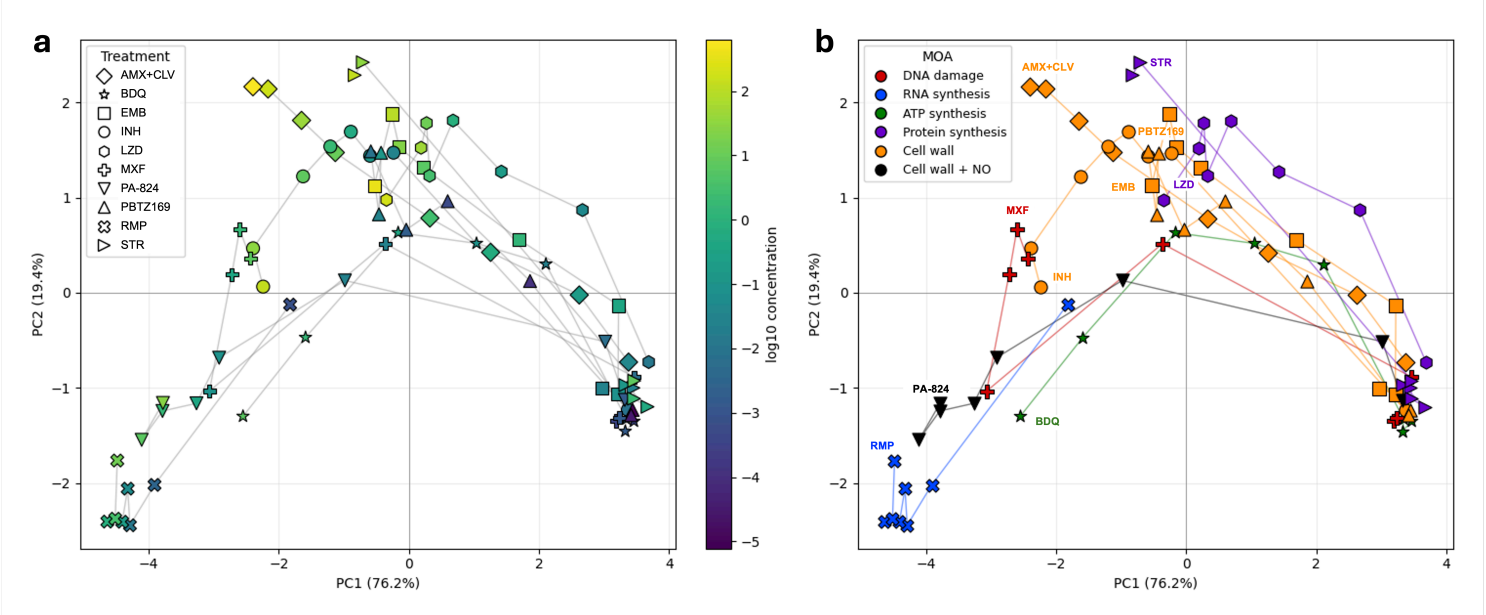

Figure 6

Integrated drug-response profiles in PCA space. a) Integrated drug-response profiles projected onto the first two principal components by drug concentration. The PCA represents the structure of the biomarker dataset at the fixed 6-day endpoint. Each point represents a single drug-concentration condition characterised by resazurin conversion, CFUs, MPNs, 16S and 23S rRNA burden, and the four RS-ratio determinations. **b)** Conditions corresponding to drugs with related MoAs tended to occupy similar regions of the PCA space.

Supplementary Files

This is a list of supplementary files associated with this preprint. Click to download.

- SuppMiniaturisedmultiplexddPCRdeterminationofrRNAbasedbiomarkerstocomplementhighthroughputMycobacteriumtuberculosisdrugresponseprofiling